Chapter 2
Spectroscopy in the Frequency Domain

Simo Huotari

2.1 Introduction

In the same way as we can not visit a distant extrasolar planet to study its properties, the atomic world lies beyond our direct reach. The human being is only capable of handling objects of a certain size—both the very large and the very small are outside of our immediate reach. In these cases we can only get information by sending probes and receiving messengers. Since the atomic world is composed of elementary particles, the natural probes and messengers are precisely elementary particles—such as photons, electrons, neutrons and atoms. In this context, by a "spectrum" we refer to an object's response to a probe as a function of probe or messenger energy (or energy loss). The experimental tool for the measurement of spectra is spectroscopy. It just happens that each one of us is equipped with a pair of eyes that are excellent visible-light spectrometers with a high energy resolution, extremely good quantum efficiency, and a large dynamic range. To achieve similar characteristics with man-made instruments turns out to be challenging. However, there are several reasons to attempt this task, from the need for extending the energy range outside the narrow region of visible light, to the convenience of using other particles besides photons. This chapter describes a few experimental spectroscopic tools that may be encountered by the user of TDDFT.

Spectroscopy is not just a tool to study the structure of atomic levels. It aims at answering the question *why* a given sample behaves as it does, e.g., why it has a certain color, or what is the driving mechanism behind possible phase transitions. Unfortunately there is no universal spectroscopy for everything. Each probing technique has its own domain of application and its own unique characteristics, such as

S. Huotari (✉)
Division of Materials Science,
Department of Physics,
P.O. Box 64, 00014 Helsinki, Finland
e-mail: simo.huotari@helsinki.fi

M. A. L. Marques et al. (eds.), *Fundamentals of Time-Dependent Density Functional Theory*, Lecture Notes in Physics 837, DOI: 10.1007/978-3-642-23518-4_2,

sensitivity either to the bulk or the surface, element specificity, and resolving power in energy, momentum, time and space.

2.2 Probe–Electron Interaction

In a spectroscopy experiment one sends a probe, which then interacts with the system. Mathematically this can be described by adding to the Hamiltonian the interaction term $\hat{H}_{\mathrm{int}}$. This causes a transition from the initial state $|\mathrm{i}\rangle$ to a final state $|\mathrm{f}\rangle$, possibly via intermediate states $|\mathrm{n}\rangle$, where the states represent the total wave functions which include the electron states (Ψ_i, Ψ_n and Ψ_f,) and those of the probe. The transition probability w is given by Fermi's golden rule which, up to second order, reads

$$w = 2\pi \left| \langle \Psi_\mathrm{f} | \hat{H}_{\mathrm{int}} | \Psi_\mathrm{i} \rangle + \sum_\mathrm{n} \frac{\langle \Psi_\mathrm{f} | \hat{H}_{\mathrm{int}} | \Psi_\mathrm{n} \rangle \langle \Psi_\mathrm{n} | \hat{H}_{\mathrm{int}} | \Psi_\mathrm{i} \rangle}{E_\mathrm{i} - E_\mathrm{n}} \right|^2 \delta(E_\mathrm{f} - E_\mathrm{i} - \omega). \quad (2.1)$$

This is the starting point for practically all spectroscopies. The differences between the various experimental techniques arise from the chosen $\hat{H}_{\mathrm{int}}$ and the set of possible Ψ_i and Ψ_f. For many applications, it is desirable that the probe wave function can be separated from the one of the target system and that the interaction $\hat{H}_{\mathrm{int}}$ is weak, so that we are in the range of validity of the Born approximation.

Scattering experiments are usually alternatively quantified by a double differential cross section (DDCS), which gives the probability of scattering of a particle with an initial energy E_1 into the solid angle element $[\Omega, \Omega + \mathrm{d}\Omega]$ and into the range of energies $[E_2, E_2 + \mathrm{d}E_2]$.

2.2.1 Photon Probe

Imagine that a photon with energy ω_1, wave vector $\boldsymbol{k}_1$, and a polarization state $\boldsymbol{\epsilon}_1$, described by the vector potential operator $\boldsymbol{A}$, interacts with an electron with a momentum operator $\boldsymbol{k}$ and an energy E_i. In the absence of an external electromagnetic field, and in the non-relativistic case, the interaction is described by the Hamiltonian (Blume 1985)

$$\hat{H}_{\mathrm{int}} = \hat{H}^{(1)}_{\mathrm{int}} + \hat{H}^{(2)}_{\mathrm{int}} + \hat{H}^{(3)}_{\mathrm{int}} + \hat{H}^{(4)}_{\mathrm{int}} \quad (2.2)$$

with the following terms:

$$\hat{H}^{(1)}_{\mathrm{int}} = \frac{\mathrm{e}^2}{2mc^2} \boldsymbol{A}^2 \quad (2.3a)$$

$$\hat{H}^{(2)}_{\mathrm{int}} = -\frac{e}{mc} \boldsymbol{A} \cdot \boldsymbol{k} \quad (2.3b)$$

$$\hat{H}_{\text{int}}^{(3)} = -\frac{e}{mc}\boldsymbol{\sigma} \cdot [\nabla \times \boldsymbol{A}] \tag{2.3c}$$

$$\hat{H}_{\text{int}}^{(4)} = -\frac{e}{2m^2c^2}\frac{e^2}{c^2}\boldsymbol{\sigma}.\left[\dot{\boldsymbol{A}} \times \boldsymbol{A}\right], \tag{2.3d}$$

where e and m are respectively the modulus of the charge and the mass of the electron, c is the velocity of light in vacuum, and $\boldsymbol{\sigma}$ is the vector of Pauli matrices. The vector potential $\boldsymbol{A}$ is linear in the creation and annihilation operators. This means that within first order perturbation theory, $\hat{H}_{\text{int}}^{(1)}$ and $\hat{H}_{\text{int}}^{(4)}$ result in scattering (two photons are involved; one in- and one out-going). On the other hand, $\hat{H}_{\text{int}}^{(2)}$ and $\hat{H}_{\text{int}}^{(3)}$ describe absorption and emission (photon number changes by one). $\hat{H}_{\text{int}}^{(2)}$ and $\hat{H}_{\text{int}}^{(3)}$ gives also rise to scattering in second order with a resonance denominator. $\hat{H}_{\text{int}}^{(3)}$ and $\hat{H}_{\text{int}}^{(4)}$ involve the spin of the electron and thus give rise to, e.g., magnetic dichroism. For most of the purposes of the discussion below these two terms will be neglected unless otherwise stated.

Inelastic scattering of a photon (or any other elementary particle) with any energy can be used to study excitations much lower in energy than the probing particle's initial energy. In the inelastic scattering process, the probe gives away an amount of energy $\omega = \omega_1 - \omega_2$ (using here the photon formalism) and momentum $\boldsymbol{q} = \boldsymbol{k}_1 - \boldsymbol{k}_2$ to the sample; $\boldsymbol{k}_2$ and ω_2 are the wave vector and the energy of the photon after the scattering process, respectively. Note that while the maximum energy transfer is ω_1, the maximum momentum transfer magnitude $q_{\max} = 2k_1$. Most commonly these inelastic scattering spectroscopies are performed with electrons (García de Abajo 2010), visible light (Raman scattering) (Devereaux and Hackl 2007), X-rays (Schülke 2007), and neutrons (Hippert et al. 2006).

The DDCS for photon scattering from terms $\hat{H}_{\text{int}}^{(1)}$ and $\hat{H}_{\text{int}}^{(2)}$, in first and second order, is

$$\begin{aligned}\frac{\mathrm{d}^2\sigma}{\mathrm{d}\Omega\,\mathrm{d}\omega_2} = r_0^2\left(\frac{\omega_2}{\omega_1}\right)\Bigg|\langle\Psi_\mathrm{f}|\mathrm{e}^{\mathrm{i}\boldsymbol{q}\cdot\boldsymbol{r}}|\Psi_\mathrm{i}\rangle(\boldsymbol{\epsilon}_1\cdot\boldsymbol{\epsilon}_2) + \frac{1}{m}\sum_\mathrm{n}\\ \times\left[\frac{\langle\Psi_\mathrm{f}|\boldsymbol{\epsilon}_2\cdot\boldsymbol{k}\mathrm{e}^{-\mathrm{i}\boldsymbol{k}_2\cdot\boldsymbol{r}}|\Psi_\mathrm{n}\rangle\langle\Psi_\mathrm{n}|\boldsymbol{\epsilon}_1\cdot\boldsymbol{k}\mathrm{e}^{\mathrm{i}\boldsymbol{k}_1\cdot\boldsymbol{r}}|\Psi_\mathrm{i}\rangle}{E_\mathrm{i}-E_\mathrm{n}+\omega_1+i\Gamma_\mathrm{n}}\right.\\ \left.+\frac{\langle\Psi_\mathrm{f}|\boldsymbol{\epsilon}_1\cdot\boldsymbol{k}\mathrm{e}^{\mathrm{i}\boldsymbol{k}_1\cdot\boldsymbol{r}}|\Psi_\mathrm{n}\rangle\langle\Psi_\mathrm{n}|\boldsymbol{\epsilon}_2\cdot\boldsymbol{k}\mathrm{e}^{-\mathrm{i}\boldsymbol{k}_2\cdot\boldsymbol{r}}|\Psi_\mathrm{i}\rangle}{E_\mathrm{i}-E_\mathrm{n}-\omega_2}\right]\Bigg|^2\delta(E_\mathrm{i}-E_\mathrm{f}+\omega).\end{aligned} \tag{2.4}$$

This is known as the Kramers–Heisenberg formula. The second term inside the brackets depends strongly on ω_1, and it only contributes significantly in the resonance condition $\omega_1 \approx E_\mathrm{n} - E_\mathrm{i}$. Indeed, it gives rise to resonant inelastic scattering. The first term describes non-resonant inelastic scattering. It is often encountered in the form

$$\frac{\mathrm{d}^2\sigma}{\mathrm{d}\Omega\,\mathrm{d}\omega_2} = r_0^2\left(\frac{\omega_2}{\omega_1}\right)(\boldsymbol{\epsilon}_1\cdot\boldsymbol{\epsilon}_2)^2 S(\boldsymbol{q},\omega) \tag{2.5a}$$

$$S(\boldsymbol{q},\omega) = -\frac{q^2}{4\pi^2 e^2}\Im\mathrm{m}\left[\epsilon^{-1}(\boldsymbol{q},\omega)\right], \tag{2.5b}$$

defining the dynamic structure factor $S(\boldsymbol{q},\omega)$ which is in turn related to the imaginary part of the inverse of the dielectric function $\epsilon(\boldsymbol{q},\omega)$.

2.2.2 Electron–Electron Scattering

When an electron scatters from another electron, it is crucial that the probe can be distinguished from the target. Thus, high-energy electrons are used as probes, with wave functions that are nearly plane waves both before ($\mathrm{e}^{\mathrm{i}\boldsymbol{k}_1\cdot\boldsymbol{r}}$) and after ($\mathrm{e}^{\mathrm{i}\boldsymbol{k}_2\cdot\boldsymbol{r}}$) the scattering event. The scattering is mediated by the Coulomb interaction $v_{\mathrm{ee}} = e^2/|\boldsymbol{r} - \boldsymbol{r}_i|$, where $\boldsymbol{r}$ and $\boldsymbol{r}_i$ are the positions of the probe and target electrons, respectively. The transition probability is (Platzman and Wolff 1973) (still denoting the energy transfer by ω)

$$w = 2\pi\left(\frac{4\pi e^2}{q^2}\right)^2 \left|\langle\Psi_{\mathrm{f}}|\mathrm{e}^{\mathrm{i}\boldsymbol{q}\cdot\boldsymbol{r}}|\Psi_{\mathrm{i}}\rangle\right|^2 \delta(E_{\mathrm{i}} - E_{\mathrm{f}} + \omega) \tag{2.6}$$

and in DDCS form

$$\frac{\mathrm{d}^2\sigma}{\mathrm{d}\Omega\,\mathrm{d}\omega} = -\frac{1}{(\pi e q)^2}\Im\mathrm{m}\left[\epsilon^{-1}(\boldsymbol{q},\omega)\right]. \tag{2.7}$$

Note the similarity between (2.5a, b) and (2.7). The main difference between electron and non-resonant photon scattering is in the kinematic prefactor, which for electrons is relatively large and scales as q^{-2}, whereas for photons it is smaller and scales as q^2.

2.2.3 Finite Momentum Transfers

In the case of X-ray and electron scattering, an important insight concerning the transition operator encountered above is given by its expansion in a Taylor series,

$$\mathrm{e}^{\mathrm{i}\boldsymbol{q}\cdot\boldsymbol{r}} = 1 + \mathrm{i}\boldsymbol{q}\cdot\boldsymbol{r} + \frac{1}{2}(\mathrm{i}\boldsymbol{q}\cdot\boldsymbol{r})^2 + \ldots \tag{2.8}$$

As the unity operator does not induce transitions, the first important term is the dipole operator $\boldsymbol{q}\cdot\boldsymbol{r}$. For optical photons, for instance, it is the only prominent term since the corresponding photon momentum q is very small and the higher order terms become negligible. Also the photon absorption operator $\hat{H}_{\mathrm{int}}^{(2)}$, even for X-rays, has

the form of a dipole operator. Note, however, that electron and X-ray scattering do not have to respect the dipole and optical limits, and q in (2.8) may be very large. For useful applications using finite q for valence and non-dipole inner-shell excitations, (see, e.g., Sternemann et al. 2005; Weissker et al. 2006; Balasubramanian et al. 2007, 2001; Huotari et al. 2010a; Sakko et al. 2010).

2.3 Properties to Study

2.3.1 Response Functions

Often there are several methods to study the same property of a given system, or quantities measured by different techniques can be otherwise related to each other. Below we consider certain well understood material-specific properties that can be probed with more than one complementary technique.

The observable of many spectroscopies can be reduced to the dielectric function. It describes the response of a dielectric material to an alternating electric field, as explained in detail in Chap. 3. We encountered this quantity already in (2.5b) and (2.7),

$$\epsilon(\boldsymbol{q},\omega) = \epsilon_1(\boldsymbol{q},\omega) + \mathrm{i}\,\epsilon_2(\boldsymbol{q},\omega). \tag{2.9}$$

The real part $\epsilon_1(\boldsymbol{q},\omega)$ gives the polarization induced by the field, and the imaginary part $\epsilon_2(\boldsymbol{q},\omega)$ describes absorption. Other optical functions (sometimes heretically called optical constants) can be deduced from the dielectric function. These include the complex refractive index $\nu + \mathrm{i}\kappa$, optical absorption coefficient α, and reflectance R. They have the relations (dependence on $\boldsymbol{q}$ and ω dropped for simplicity)

$$\epsilon_1 = \nu^2 - \kappa^2 \quad \epsilon_2 = 2\nu\kappa \quad \alpha = 4\pi\kappa\omega/c \tag{2.10a}$$

$$\nu = \left[\left(\sqrt{\epsilon_1^2 + \epsilon_2^2} + \epsilon_1\right)/2\right]^{1/2} \quad R = \frac{(\nu-1)^2 + \kappa^2}{(\nu+1)^2 + \kappa^2} \tag{2.10b}$$

For instance, the absorption coefficient α is used when considering the transmittance of a sample, which is described by the Beer–Lambert law,

$$I_1 = I_0 \mathrm{e}^{-\alpha d}, \tag{2.11}$$

telling us that if the intensity of light is initially I_0, it has decreased to a value I_1 after passing through a sample that has a thickness d. Inelastic scattering techniques, in turn, measure the loss function, which we in fact already quietly introduced in (2.5b) and (2.7),

$$L(\boldsymbol{q},\omega) = -\Im\mathfrak{m}\left[\frac{1}{\epsilon(\boldsymbol{q},\omega)}\right] = -\frac{\epsilon_2(\boldsymbol{q},\omega)}{[\epsilon_1(\boldsymbol{q},\omega)]^2 + [\epsilon_2(\boldsymbol{q},\omega)]^2}. \tag{2.12}$$

The real and imaginary parts of the dielectric function can be retrieved from loss-function measurements using the Kramers–Kronig relations,

$$\Re\mathfrak{e}\left[\epsilon(\boldsymbol{q},\omega)^{-1}\right] = 1 + \frac{1}{\pi}\mathcal{P}\int \frac{\mathrm{d}\omega'}{\omega'-\omega}\Im\mathfrak{m}\left[\epsilon(\boldsymbol{q},\omega)^{-1}\right] \tag{2.13a}$$

$$\Im\mathfrak{m}\left[\epsilon(\boldsymbol{q},\omega)^{-1}\right] = -\frac{1}{\pi}\mathcal{P}\int \frac{\mathrm{d}\omega'}{\omega'-\omega}\Re\mathfrak{e}\left[\epsilon(\boldsymbol{q},\omega)^{-1}-1\right], \tag{2.13b}$$

where $\mathcal{P}$ denotes the Cauchy principal value of the integral. Optical spectroscopies measure essentially the limit $\epsilon(0,\omega)$ because the optical photon momentum is practically zero. This is not a limitation for electron and X-ray spectroscopies since in those cases momenta can be very large—recall Sect. 2.2.3.

2.3.2 Typical Excitations

Excitations can be seen in the frequency-dependent linear response, and hence in the density-density response function as discussed in Chap. 4. A few examples of excitations that will be encountered in the applications of TDDFT are shown schematically as a loss function spectrum in Fig. 2.1.

- The infrared (IR) range includes vibrational excitations (phonons), and can be studied via IR absorption or high-resolution inelastic scattering techniques. For electronic excitations, the typical example in this region is free-carrier (electrons or holes) absorption. Electrical properties such as conductivity and carrier concentration can be then studied.
- Spin excitations (magnons) (100–500 meV), studied typically by neutrons (Hippert et al. 2006), due to the coupling of the magnetic moments of the neutron probe and the target atom, or resonant inelastic X-ray scattering (Ament et al. 2011).
- Valence spectra including excitations across the band gap in semiconductors (up to a few eV), excited by visible- or ultraviolet (UV) light absorption or Raman scattering, are routinely studied with TDDFT (Albrecht et al. 1998) and are treated in detail in this book.
- Collective plasmon modes [a few meV for ISB plasmons in semiconductor nanostructures (Ullrich and Vignale 2001), or several eV in bulk condensed matter (Weissker et al. 2006)]. Plasmons can also be seen in photoemission spectra as satellite peaks due to extrinsic energy losses of measured photoelectrons.
- Inner-shell-electron excitations ($\gtrsim$100 eV) (Stöhr 1992).
- Compton recoil scattering, that yields information on the ground-state momentum density (Cooper et al. 2004).

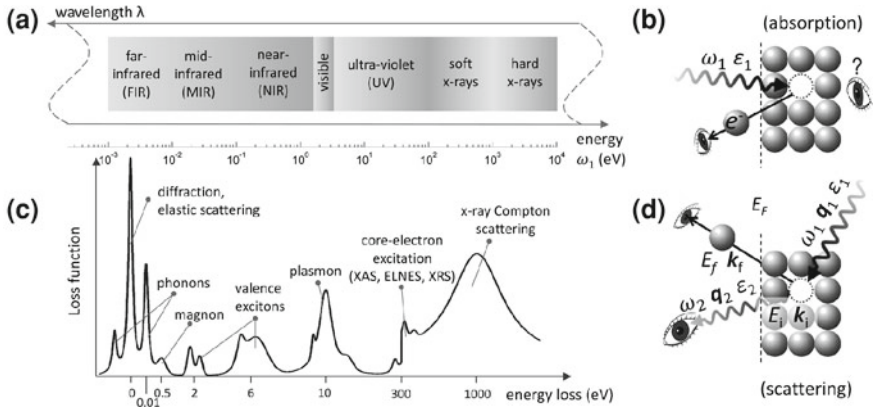

Fig. 2.1 **a** The spectrum of electromagnetic radiation in the regions of vibrational and electronic excitations. **b** An excitation of an electron above the Fermi level E_F in a photoabsorption process. **c** The different excitations that can be revealed by the loss function. **d** An inelastic scattering experiment, shown here for photons

2.4 Techniques

2.4.1 Ellipsometry

Ellipsometry (Fujiwara 2007; Tompkins and McGahan 1999) is a powerful tool for measuring $\epsilon(0, \omega)$ in solids, especially for surfaces and thin films. The true power of ellipsometry is that both real and imaginary parts are obtained simultaneously and independently, without the need to resort to Kramers–Kronig analysis. The readers of this book will encounter examples of ellipsometric data in many of the following chapters, e.g., the optical spectra of silicon of (Lautenschlager et al. 1987). The ellipsometric measurement analyzes the change of light polarization when it is reflected by the sample surface or transmitted through the sample. The photon energies range from IR to UV.

The name of the technique derives from the fact that the measured light is in general elliptically polarized, and it is this degree of polarization that is determined in the experiment. Namely, it measures the ratio of the reflectances of polarization components perpendicular and parallel to the sample surface, denoted R_s and R_p, respectively. This ratio is given usually as an amplitude and phase shift, denoted $\tan(\Psi)$ and Δ respectively, i.e., $R_p/R_s = \tan(\Psi)e^{i\Delta}$.

A typical example of an ellipsometry measurement is a three-phase model of an ambient—thin film—substrate ensemble. In this kind of system, ellipsometry can measure the thickness and optical properties of the thin film, assuming the substrate's optical properties are well known in advance. On the other hand, the same model is often used to study any substrate that has an oxide over-layer. The dielectric function is not directly measured by the ellipsometry experiment. Its extraction from the

measured data requires the use of certain computational models and it is not possible to give the relation of the dielectric function and the measured quantity of R_p/R_s in a closed form. Thanks to the advancements in computing power and the consequent automatization and commercialization of ellipsometry instruments since the 1990s, the technique has become rather popular.

2.4.2 Photoemission Spectroscopies

Photoemission spectroscopy (PES, or XPS for X-ray photoemission spectroscopy) has a long and successful history. A good review on the subject is, e.g., Hüfner (2007). Since Hertz discovered the photoelectric effect in 1887, Einstein was awarded the Nobel Prize in 1921 for its explanation, and Kai Siegbahn in 1981 for its use as an analytical tool. A large part of our current understanding of the electronic structure of materials is due to photoemission spectroscopy. The relatively straightforward interpretation of the measured results and their direct connection to the electronic structure has provided a good basis for photoemission to become a standard research tool.

In a photoemission experiment, a photon with energy ω_1 impinges on a sample; ω_1 can belong to the UV range (produced with a discharge lamp) up to X-rays (produced by a X-ray tube or a synchrotron). The photon gets absorbed ($\hat{H}_{\rm int}^{(2)}$) and removes a photoelectron which can be detected and its kinetic energy E_K measured by an electrostatic analyzer. From the measurement of E_K and the knowledge of the photoelectron direction, the full photoelectron momentum vector $\boldsymbol{k}$ is obtained. The original binding energy E_B of the electron before emission can be obtained from the photoelectric equation:

$$E_K = \omega_1 - \phi - |E_{\rm B}|, \tag{2.14}$$

where the work function ϕ is the energy required for electrons to escape the material surface, typically of the order of 4–5 eV for metals. Note that in the PES jargon, the values for $E_{\rm B}$ are usually taken to be positive, and $E_{\rm B} = 0$ at the Fermi energy $E_{\rm f}$.

In a solid-state sample we have to consider both the valence band and core levels. Due to higher resolving power in $\boldsymbol{k}$ and $E_{\rm B}$, valence-band studies are usually done with UV-excitation ultra-violet photoemission spectroscopy (UPS) or very low-energy X-rays. Core levels require X-ray excitation, because to access a given $E_{\rm B}$ requires naturally $\omega_1 > E_{\rm B} + \phi$.

The final state of a photoemission process involves an electron removed completely from the system, and the sample is left with a positive total charge. The hole left behind interacts strongly with the rest of the sample, and thus the final state is in fact quite complex. The description of PES can be first of all simplified by the so-called sudden approximation, in which one assumes that the final state electron does not interact anymore with the hole left behind or with the other electrons of the sample. This makes it possible to factorize the photoelectron wave function from the

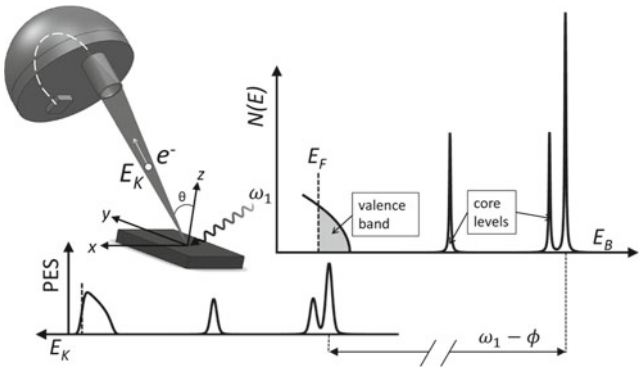

Fig. 2.2 PES experiment. The measured PES as a function of the electron kinetic energy E_K corresponds to the occupied density of states $N(E_B)$ of the electron system

wave function of the system of the other $N-1$ electrons. Furthermore, one usually divides the photoemission process into three independent and sequential steps. This is known as the three-step model (Hüfner 2007): (i) Excitation of the photoelectron within the sample, i.e., the transition between the ground and an excited Bloch state within the solid $\Psi_{\mathrm{i}}^{\boldsymbol{k}_{\mathrm{i}}}$ and $\Psi_{\mathrm{f}}^{\boldsymbol{k}_f}$. If the photon momentum is neglected, they both share the momentum $\boldsymbol{k}_{\mathrm{i}} = \boldsymbol{k}_{\mathrm{f}} = \boldsymbol{k}$. This step is quantified by $M_{\mathrm{f,i}}^{\boldsymbol{k}} = \langle \Psi_{\mathrm{f}}^{\boldsymbol{k}} | \hat{H}_{\mathrm{int}}^{(2)} | \Psi_{\mathrm{i}}^{\boldsymbol{k}} \rangle$. (ii) Electron propagation to the surface. (iii) Escape from the surface to the vacuum. The total PES intensity is then given by the product of probabilities for these individual processes. All information on the electronic structure of the ground state is contained in the step (i). Step (ii) depends on the mean free path of the electron in the solid. The probability for step (iii) depends on E_K and Ψ. The PES can be reduced to (Hüfner 2007; Damascelli et al. 2003)

$$\mathrm{PES} \propto \sum_{\mathrm{f,i}} \left| M_{\mathrm{f,i}}^{\boldsymbol{k}} \right|^2 A(\boldsymbol{k}, E) \delta \left(E_K + E_{\mathrm{f}}^{N-1} - E_{\mathrm{i}}^{N} - \omega_1 \right), \tag{2.15}$$

where $A(\boldsymbol{k}, E) = \sum_m |\langle \Psi_m^{N-1} | \hat{c}_{\boldsymbol{k}} | \Psi_{\mathrm{i}}^{N} \rangle|^2$ and $\hat{c}_{\boldsymbol{k}}$ is the destruction operator of an electron of momentum $\boldsymbol{k}$. The function A is called the spectral function and describes the PES spectrum, since usually one considers the matrix elements $M_{\mathrm{f,i}}^{\boldsymbol{k}}$ to be constant throughout the PES measurement. In the non-interacting-particle picture $A(\boldsymbol{k}, E)$ reflects the occupied density of electron states by being a series of peaks located at the single-particle orbitals with energies E_{B}, schematically shown in Fig. 2.2. The calculation of photoemission spectra is discussed more in detail in Chap. 3.

Angle-resolved PES (**ARPES**) (Damascelli et al. 2003) could as well be called band-resolved PES. With a small kinetic energy of photoexcited valence electrons it is possible to achieve a very high resolution in both their binding energy and initial momentum, thus mapping effectively the occupied band structure $E(\boldsymbol{k})$. ARPES is a very powerful and a direct tool for studying the electronic structure of the surface

of solids. Since the photon momentum can be neglected in the UV-range typically used in ARPES, the electron momentum is conserved for the in-plane component $k_{||} = \sqrt{2mE_K}\sin\theta$.

Hard-X-ray PES (**HAXPES**) (Horiba et al. 2004; Panaccione et al. 2006) differs from traditional UPS and XPS by using hard X-rays ($\omega_1 \gtrsim 5\,\mathrm{keV}$). PES is usually highly surface-sensitive and as such a great tool for studying the electronic structure of the surfaces of solids. For gaining access to information on the bulk electronic states, one can utilize the fact that the electron mean free path increases with increasing kinetic energy when working in the X-ray region. Probing depth can be increased to 15–20 nm with $\omega_1 \approx 6\,\mathrm{keV}$, compared to 0.5–1 nm in UPS. The disadvantage is a lower cross section and the requirement of a synchrotron laboratory as a light source.

Inverse photoemission (**IPES**) probes instead the unoccupied states. If an electron with an initial kinetic energy E_K impinges on the sample and fills an unoccupied state with an energy E_{unocc}, a photon with an energy $E_K - E_{\mathrm{unocc}}$ may be emitted and detected. From the measurement of the IPES intensity as a function of the photon energy, the density of unoccupied states can be deduced. The technique can also be called Bremsstrahlung isochromate spectroscopy (BIS) especially if photons are detected with a fixed energy $E_K - E_{\mathrm{unocc}}$ and the energy of incident electrons E_K is varied. A typical example of a combination of PES and BIS is that of the determination of the band gap of NiO (Sawatzky and Allen 1984).

2.4.3 Photon Absorption

Absorption spectroscopy measures how well a sample absorbs or transmits electromagnetic radiation at a given range of photon frequencies. Photoabsorption is a result of the same $\hat{H}^{(2)}_{\mathrm{int}}$ as photoemission, but now the electron is not removed from the sample. It is merely lifted to an unoccupied state above the Fermi level. The electron stays within the vicinity of the created ion and feels the presence of the core hole; the electron-hole interaction has thus to be explicitly included in any theoretical description. When a sample absorbs a photon with energy ω_1, an excitation with that particular energy is created—the relevant energy ranges are depicted in Fig. 2.1a. For experimentalists, the hugely different energy ranges mean different practicalities and the measurement techniques vary greatly.

Circular dichroism (**CD**) (Berova et al. 1994) is an effect where the absorption coefficient is different for left (−) and right (+) circularly polarized light. This is typically observed in the optical response of chiral molecules, where the response to the different circular polarization depends on the handedness of the molecule. In the X-ray regime, an effect with a similar name (magnetic CD) is due to the interaction Hamiltonian $\hat{H}^{(3)}_{\mathrm{int}}$. It is used to probe the difference in the unoccupied electron states bearing different spin, giving access to the orbital magnetic moment (Thole et al. 1992; Lovesey and Collins 1996). A CD measurement is very similar to a regular

absorption measurement, and only differs in one way: the incident photon beam is circularly polarized, and the transmitted intensity is measured for two different polarizations. The CD signal is then the relative difference of the transmitted intensities for the two polarizations, $(I_+ - I_-)/(I_+ + I_-)$.

Infrared absorption probes excitations in the meV-range. Many of them are vibrational in character. IR spectroscopy is often used to identify molecules via their well-characterized vibrational excitations. They are superimposed on the spectra of low-lying electronic excitations such as magnetic excitations or electron excitations in nanostructures that have energies in the sub-eV range. The majority of IR absorption instruments are Fourier-transform spectrometers, which are able to collect spectra over a wide energy range simultaneously. Complementary probes for the same excitations in this energy range can be found within the Raman and resonant-Raman spectroscopies and inelastic neutron spectroscopy.

UV-visible absorption (**UV/Vis**) covers typically excitations of 3d electrons in transition metals, important for studies of strongly correlated oxides, and band gaps in semiconductors. Also many organic molecules also absorb light in the UV/Vis range. Excitations in this regime may also be studied with inelastic X-ray and electron scattering spectroscopies via the loss function.

X-ray absorption (**XAS**) (Stöhr 1992) is one of the most common X-ray spectroscopies and TDDFT has much to offer in this field (Brancato et al. 2008). The largest difference between X-ray and optical absorption studies is that in XAS the initial electron state is a dispersionless, narrow, and deeply bound core state. This partly facilitates the analysis of the spectra since to a rather good approximation they measure the unoccupied states directly, although always in the presence of the deep core hole and broadened by the core hole lifetime. Even more importantly, XAS is element specific due to the involvement of the core state, and can thus be used as an accurate tool even in many otherwise complex systems. XAS is a quite recent addition to the spectroscopy family since tunable X-ray sources have been recently introduced with the advent of synchrotron radiation. Depending on the sample and the range of X-ray energies, the experiments can be performed by measuring the ratio of the transmitted and incident photon intensities, or indirectly, by observing consequent processes such as secondary-particle yield (e.g., Auger processes or photoemission). The fine structure of the spectra near the edge X-ray absorption near-edge structure (XANES), yields information on the local electron density of unoccupied states at the site of the absorbing atom, in the presence of the core hole. At increasingly larger photon energies, the photoelectron has more kinetic energy and can probe also the surrounding environment by scattering from the neighboring atoms. This gives rise to extended X-ray absorption fine structure (EXAFS), which exhibits characteristic oscillations due to the interference of the outgoing and backscattered photoelectron wave functions. After expressing the oscillations as a function of the photoelectron momentum, a Fourier transformation of the signal gives information on the

neighboring atoms in a form of an effective pair distribution function (Rehr and Albers 2000). Complementary probes to XAS can be found from inelastic scattering of electrons and X-rays.

2.4.4 Inelastic Scattering

Originally V. Raman noted that it was possible to measure vibrational excitations, which have energies that fall into the far-infrared regime, by observing characteristic energy losses in the spectrum of visible light. For this finding he was awarded the Nobel prize in 1930. The effect was immediately realized to be due to inelastic light scattering. For light this is possible only in the particle picture (Nobel prize of A. H. Compton 1927), and indeed inelastic scattering is a property of particles (neutrons and electrons are canonical examples). An important difference to absorption is that inelastic scattering allows investigations of a possible q-dispersion of the excitations.

Raman spectroscopy (Devereaux and Hackl 2007) is complementary to IR absorption, and is often used in the studies of vibrational and electronic excitations in the meV-energy range in molecules and solids. Its flavor called resonant-Raman spectroscopy allows to distinguish between charge-density, spin-density, and single-particle excitations. In resonant Raman experiments, the energy of the incident photon is tuned to a specific electron excitation (often to that of a band gap), and other low-energy excitations coupled to the resonance gain spectral weight considerably. This is especially useful in complex systems where certain classes of excitations can be selectively studied.

Electron-energy loss spectroscopy (EELS) and electron microscopy (García de Abajo 2010) are widely used and powerful tools to study the electronic properties, especially of thin films and surfaces with a very high spatial resolution. Due to the large electron-electron scattering cross section, the measurements are fast and high resolving power is easy to achieve in all quantities: energy, momentum transfer, and space—in particular, electrons are very easy to focus on nm-size spots on the sample. There are several different types of electron spectroscopy. The transmission electron microscope (TEM) uses high-energy electrons that are made to pass through a thin (≤ 100 nm) sample film, or a gas. Measuring the energy loss of the electrons measures essentially the loss function $L(\boldsymbol{q}, \omega)$ as discussed in Sect. 2.3. Inelastic electron scattering gives rise to cathodoluminescence (CL) (Ozawa 1990) which can be measured and analyzed in the scanning electron microscope (SEM). CL was also produced in the old-fashioned cathode-ray tubes, such as television sets and computer monitors, before the flat-screen revolution. Just as PES, EELS can be used in chemical analysis by measuring the core-electron excitations (Hitchcock 2000). This flavor of EELS is sometimes called energy-loss near edge spectroscopy (ELNES), yielding similar information as XAS. EELS is a useful probe for both bulk and surface excitations which are both typically present in the measured spectra. The

large scattering cross section, especially at low q values, can sometimes be a disadvantage due to the large possibility for multiple scattering. This is well known in solids (Bertoni and Verbeeck 2008; Stöger-Pollach 2008), but should also be carefully considered even in gases (Bradley et al. 2010).

Inelastic X-ray scattering spectroscopy (IXS) (Schülke 2007) can also be used to study the loss function $L(\boldsymbol{q}, \omega)$. Historically, the first observation of the IXS process was the well-known Compton effect, where X-rays scattered off a sample suffer a shift in wavelength, $\Delta\lambda = \frac{h}{mc}(1 - \cos 2\theta)$; the scattering angle 2θ is the angle between the incident and scattered photon. This effect is due to recoil scattering from the electrons. The scattering electron is usually not at rest, and its ground-state momentum gives an additional Doppler shift to the recoil photon. By measuring the Compton-recoil IXS spectrum, the ground state initial momentum of the electron can be deduced (Cooper et al. 2004; Huotari et al. 2010b). The Compton spectrum can be obtained from $L(\boldsymbol{q}, \omega)$ measured at large q. IXS studies of the loss function at smaller values of q have recently advanced to the level of a standard tool due to the fact that monochromatic and energy-tunable X-rays with high enough intensity can only be produced by modern synchrotron radiation facilities. The difference between IXS and EELS arises mostly from a much larger scattering probability in EELS especially at small q. This has made EELS experiments often faster, and has for a long time limited IXS to low-Z systems, where the large probing depth compensates the low cross section. However, modern high-brilliance synchrotron radiation sources have now made IXS experiments possible in all samples. IXS has the advantages of (i) being bulk-sensitive, yielding access also to samples in environments impermeable for electrons which scatter already at the surface of materials, and (ii) being able to perform measurements for an almost unlimited range of momentum transfers, only limited by $q_{\max} = 2k_1$. The ELNES counterpart for inner-shell excitations in IXS is called X-ray Raman spectroscopy (XRS)—a name which describes well the inelastic process but is not to be confused with optical Raman spectroscopy. Just as in the case of resonant-Raman spectroscopy, it is possible to perform IXS in resonant conditions in a resonant inelastic X-ray scattering (RIXS) spectroscopy experiment. In this case $\omega_1 \approx E_\mathrm{i} - E_\mathrm{n}$ and the second term under the square in the DDCS (2.4) dominates (Ament et al. 2011). Now the intermediate state Ψ_n corresponds to the final state in XAS—i.e., a deep core hole and an extra electron in a previously unoccupied valence state. The involvement of an intermediate state lifts off many selection rules such as the dipole rule. RIXS is element specific due to the involvement of the core hole, and thus used often in complex samples where the local electronic structure of a specific element is studied. Typical applications are strongly correlated systems, e.g., charge-transfer excitations in transition metal oxides (Schülke 2007).

Inelastic neutron spectroscopy (INS) (Hippert et al. 2006) is a widely used probe for phonons and magnetic excitations (magnons), as well as crystal field excitations within partially filled d or f electron shells. Phonons are excited in INS due to the neutron-nucleus interaction and magnetic excitations due to the magnetic-moment coupling of neutrons and atoms. The spectra are usually expressed in terms of the dynamic structure factor $S(\boldsymbol{q}, \omega)$. The nuclear scattering probability is represented

by the scattering length b, which is not a monotonic function of the target atomic number, and depends also on the isotope. INS is a well established tool for phonon and magnon measurements, recently also complemented by IXS (Scopigno et al. 2005) and RIXS (Ament et al. 2011).

2.4.5 Non-linear Optics

Non-linear optics is thoroughly reviewed in Chap. 18. In this case the first Born approximation does not apply, since the polarization caused by the probe is comparable to the field of the probe itself. This may lead to rather unexpected phenomena, such as high-harmonic generation which makes the sample to respond at multiples of the initial probe frequency (Salières et al. 1999). These techniques constitute a rapidly evolving field. Its latest additions are in the X-ray regime thanks to the advent of X-ray free electron lasers, which could very well turn out to be the light sources of the future for spectroscopists.

2.5 Summary

There is a large number of open questions in physics that spectroscopy could answer in near future. Some of the most important ones relate to many-body effects, and the lack of exact functionals to account for them. Especially strong electron-electron interaction effects for instance are manifested in low-dimensional systems—i.e., in the nanoscale. The understanding of strongly correlated systems is one of the forefront questions in the contemporary condensed matter physics and experimental results are often difficult to interpret without an ab initio theoretical counterpart. Such systems are often probed by resonant spectroscopies such as resonant inelastic X-ray scattering, where the development of rigorous ab initio theories has been especially slow. Also, the interpretation of the behavior of disordered matter such as glasses and liquids has been more difficult than those of crystalline systems due to their lack of periodicity.

Luckily spectroscopy is a large field that is developing on a fast pace. As is the case generally in science, spectroscopic experiments and theory are in a constant dialogue. Improvements in one always lead to a surge of advances in the other as a response. Sometimes experimentalists discover new phenomena with no obvious theoretical explanation, forcing the theorists to improve their techniques in the search for one. On the other hand, theoretical predictions have been made for experimentally previously unseen phenomena that have demanded a completely new level of accuracy from experiments in order to be confirmed. In the twenty first century, our understanding of physics will probably be revolutionized due to the advent of powerful new techniques and light sources allowing novel spectroscopic studies in previously inaccessible time and energy scales.

http://www.springer.com/978-3-642-23517-7

Fundamentals of Time-Dependent Density Functional Theory

Marques, M.A.L.; Maitra, N.T.; Nogueira, F.M.S.; Gross, E.K.U.; Rubio, A. (Eds.)

2012, XXXII, 559 p. 72 illus., Softcover
ISBN: 978-3-642-23517-7